Since January 2020 Elsevier has created a COVID-19 resource centre with free information in English and Mandarin on the novel coronavirus COVID-19. The COVID-19 resource centre is hosted on Elsevier Connect, the company's public news and information website.

Building and Environment 107 (2016) 154–168

Contents lists available at ScienceDirect

Building and Environment

journal homepage: www.elsevier.com/locate/buildenv

Airflow patterns through single hinged and sliding doors in hospital isolation rooms – Effect of ventilation, flow differential and passage

Petri Kalliomäki [a, b, *], Pekka Saarinen [a, b], Julian W. Tang [c, d], Hannu Koskela [a, b]

[a] Finnish Institute of Occupational Health, Lemminkäisenkatu 14 – 18 B, 20520 Turku, Finland
[b] Turku University of Applied Sciences, Lemminkäisenkatu 14 – 18 B, 20520 Turku, Finland
[c] Clinical Microbiology, University Hospitals of Leicester, United Kingdom
[d] Department of Infection, Immunity and Inflammation, University of Leicester, Leicester, United Kingdom

ARTICLE INFO

Article history:
Received 11 April 2016
Received in revised form
3 June 2016
Accepted 13 July 2016
Available online 15 July 2016

Keywords:
Isolation room
Containment failure
Door operation
Airborne infection
Full-scale experiments
Passage

ABSTRACT

Negative pressure isolation rooms are used to house patients with highly contagious diseases (e.g. with airborne diseases) and to contain emitted pathogens to reduce the risk for cross-infection in hospitals. Airflows induced by door opening motion and healthcare worker passage can, however, transport the potentially pathogen laden air across the doorway. In this study airflow patterns across the isolation room doorway induced by the operation of single hinged and sliding doors with simulated human passage were examined. Smoke visualizations demonstrated that the hinged door opening generated a greater flow across the doorway than the sliding door. Tracer gas measurements showed that the examined ventilation rates (6 and 12 air changes per hour) had only a small effect on the air volume exchange across the doorway with the hinged door. The results were more variable with the sliding door. Supply-exhaust flow rate differential reduced the door motion-induced air transfer significantly with both door types. The experiments showed that the passage induced substantial air volume transport through the doorway with both door types. However, overall, the sliding door performed better in all tested scenarios, because the door-opening motion itself generated relatively smaller air volume exchange across the doorway, and hence should be the preferred choice in the design of isolation rooms.

1. Introduction

Patients with highly infectious airborne diseases are typically placed in negative pressure isolation rooms to prevent the spreading of pathogens to adjacent spaces, hence reducing the risk of cross-infection. Droplets and particles of different sizes are released from breathing, coughing, or sneezing [1,2]. After release these particles and droplets undergo evaporative water loss in the air to become droplet nuclei [3]. However, large particles (diameter >20 μm) may rapidly deposit onto wall surfaces because the force of gravity is more significant than ventilation induced effects. Smaller particles (0.1–10 μm) may be suspended for a long time though and contribute to disease transmission over great distances [4]. Thus fine particles and gaseous pathogens are significantly influenced by ventilation and airflow patterns.

Typically mixing ventilation with sufficiently high ventilation rates (6–12 air changes per hour, ACH) are recommended for isolation rooms for quick and effective dilution [5–8]. The negative pressure in negative pressure isolation rooms draws the air towards the isolation room in order to minimise the leakage of potentially contaminated air into surrounding areas. However, the situation can be disrupted by many factors which can lead to containment failure [9,10], including: the opening of the doors themselves, which cancels or even reverses the negative pressure between the rooms, allowing the escape of potentially contaminated air through the open doorway [11]; the passage of healthcare workers through the doorway, which increases the airflow through the doorway as moving body creates a wake in which air and contaminants can be transported over long distances [12–16], e.g. out of isolation room [17–20]. It has been estimated that the combined effect of door opening and passage may be among the most important factors causing containment failures in isolation rooms [9,10].

Following the severe acute respiratory syndrome (SARS) outbreaks of 2003 and the subsequent concerns about avian A/H5N1,

* Corresponding author. Turku University of Applied Sciences, Lemminkäisenkatu 14 – 18 B, 20520 Turku, Finland.
E-mail addresses: petri.kalliomaki@turkuamk.fi, petrikal82@gmail.com (P. Kalliomäki).

http://dx.doi.org/10.1016/j.buildenv.2016.07.009
0360-1323/

pandemic A/H1N1pdm09 influenza, and most recently Middle East Respiratory Syndrome-associated coronavirus (MERS-CoV) viruses, negative pressure isolation rooms are now extensively used in hospitals, worldwide. Enhanced usage has led to increased interest in containment testing and to door operation induced air and contaminant transport [19–34]. A wide variety of different methods have been used to study the issue, including: computational fluid dynamics (CFD) [23,26,30–32,34], small-scale models [19,22,24,29], full-scale models [20] and field studies [21,25,27,28,32,33].

Regardless of the methods used, most of the studies have concentrated on the single hinged door-generated airflows [21–25,27–29,31–33] and only a few of the recent studies have experimentally examined the differences between hinged and sliding doors [19,20], although the differences between the two door types have not always been clear. For instance, some earlier studies have shown that the usage of sliding doors can reduce the airflow out of the isolation rooms compared to hinged doors [17,35]. On the other hand, it has been argued also that there are no significant differences on the isolation efficiency [36] or on the air volume migration generated by the operation the two door types [18]. However, more recent studies have shown experimentally that sliding doors can reduce the air exchange through the doorway [19,20]. Nevertheless, more evidence and data are needed on the range of door-opening-induced flows with and without passage under realistic isolation room conditions (e.g. ventilation rates, supply-exhaust flow rate differential etc.) to clarify the differences between sliding and hinged doors.

This article extends the scope of the previously published baseline papers by Tang et al. [19], Kalliomäki et al. [20] and Saarinen et al. [23] in which the authors studied the isolation room door operation induced airflows with small-scale water, full-scale air and CFD models without ventilation. This paper takes these experiments a step further and examines the effect of realistic ventilation rates, supply-exhaust flow rate differential and simulated human passage on the airflow patterns and air volume exchange across the isolation room doorway generated by hinged and sliding doors.

2. Methods

2.1. The full-scale isolation room model

The experiments were carried out in a full-scale isolation room model. The model was built out of clean room elements into a larger laboratory space (see Fig. 1). The model consisted of two identical and adjacent rooms (each 4.0 m long, 4.7 m wide and 3.0 m high) connected with a door in the middle of a central, dividing wall. In the model, Room 1 was designated as an anteroom and Room 2 as an isolation room (see Fig. 1 for further details). Interior of the model was painted black (see Fig. 2) to enhance the visibility of the smoke during smoke visualizations. The experiments were carried out for two different door types, first with a single hinged door (opening towards Room 2) and then for a sliding door (mounted on Room 1 side of the doorway). The doorway was 2.06 m high and 1.10 m wide with both door types.

Passage through the doorway was simulated with a moving manikin (without any surface heating, so there was no thermal plume present). The manikin was 1.7 m tall and was wearing a laboratory robe to simulate the outfit of hospital staff. The manikin was fixed to a small cart (on wheels) moving along a rail running on the floor between the two rooms (see Fig. 2). The movements of the manikin and the door were controlled by the same computer program, making the synchronization of the door movements and manikin passage easier and repeatable throughout the experiments.

Fig. 3 shows the details of the door and manikin movement cycles. Initially, the manikin stood in the middle of a room. As the cycle began, the manikin accelerated rapidly to full-speed (1 m/s), approached the door and stopped in front of it. After the door had opened completely, the manikin moved through the doorway into the other room. The manikin stopped at the center of the other room and following a short wait the door closed behind the manikin after which the moving cycle was considered to be over. In each examined case the door opened in 3 s, stayed fully open for 8 s and closed in 5.4 s. The hold-open time was set long enough for the manikin to pass through the doorway avoiding crashing with the door. During the hinged door experiments the manikin halted slightly further away from the door (while approaching it from the isolation room side) to avoid collision with the sweeping door. Otherwise, the door-manikin movement cycles were similar for the experiments with both door types.

Mixing ventilation was used throughout the experiments as it is recommended for isolation rooms by several guidelines [5–8]. Although there have been efforts to locate the ideal positions of the supply and exhaust registers the optimal setting is still somewhat unclear [37,38]. One suggested choice is top-supply-top-exhaust [5,6,38] and hence it was decided to install a radial supply air diffusers in the ceiling at the center of the rooms and rectangular exhaust grilles (280 mm × 180 mm) up on the wall close to the ceiling next to the dividing wall in both rooms (see Fig. 1 for details). The diffuser outlet section pointing towards the doorway was blocked in order to avoid direct flow to door as this might severely affect the doorway flows possibly increasing the risk for

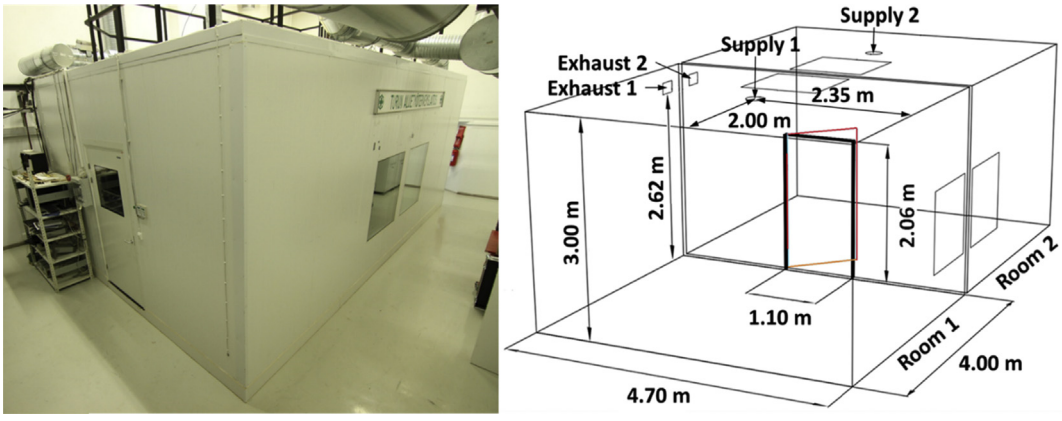

Fig. 1. Full-scale isolation room model used in the experiments and its layout.

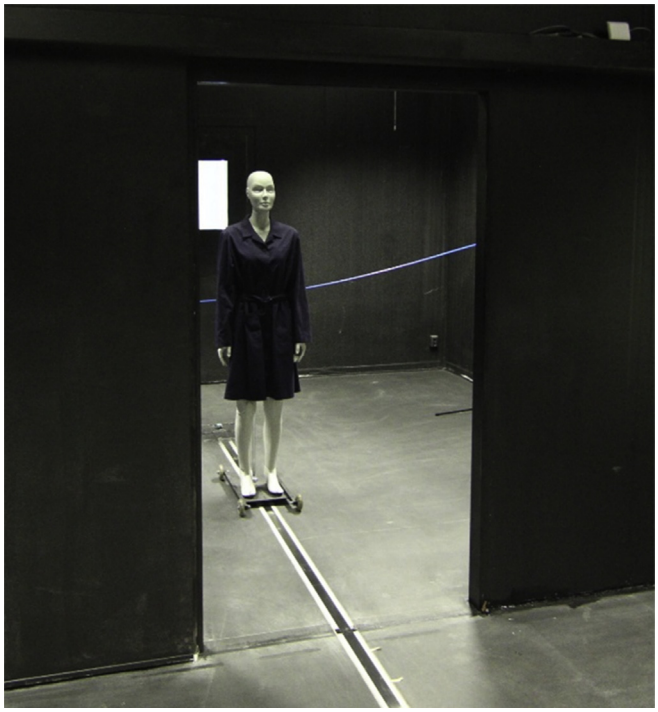

Fig. 2. The isolation room model seen from inside.

containment failures. Two air change rates (based on exhaust flow rates) were used in the study, 6 and 12 ACH (corresponding flow rates being 94 and 188 L/s). Supply air temperature was set the same in both rooms resulting in ~22 °C room temperature. The supply and exhaust airflow rates and the pressure difference between the rooms were monitored and measured with Swema 3000 multi-purpose instrument (Swema, Sweden). Calibrated orifices were installed to the supply and exhaust ducts for accurate airflow rate measurement. The accuracy for airflow rate measurement was ±4 L/s and for pressure ±0.3 Pa. The room temperatures were monitored continuously with thermometers (Craftemp thermistors, Craftemp, Sweden, ±0.2 °C accuracy) located at 1 m and 2.6 m above the floor in each room.

2.2. Smoke visualizations

2.2.1. Experimental methods

Smoke visualizations were carried out to demonstrate the flow patterns across the doorway induced by the hinged and sliding doors and the manikin passage. Theatre smoke was produced with a smoke generator (Martin Magnum 550, Martin Pro-Smoke Super ZRMix fluid, Martin, Denmark). This produced thick yet buoyant smoke suitable for airflow pattern visualization. The particle size distribution of the smoke was not measured, but according to the manufacturer's product document [39] it is around 1–1.5 μm, corresponding to fine particles whose dispersion process is similar with gaseous agents and hence suitable for airflow visualizations.

The smoke generator was positioned outside the isolation room model to avoid unnecessary heat sources inside the mock-up. The smoke was dosed through a hose in which the smoke cooled down before entering the model. Only one of the rooms was filled at a time. The smoke was quickly and uniformly mixed inside the room due to effective mixing ventilation.

In the empty room (smoke free in the beginning), a vertical or a horizontal sheet was illuminated. The vertical sheet (door wide, narrowing towards the lights) was used for side-view illumination and the horizontal sheet (between 0.6 and 1.4 m above the floor also narrowing towards the lights) for top-view illumination of the smoke. Altogether, the visualizations were recorded from four different angles (side- and top-view on each room) in separate, consecutive experiments, as only one camera (Canon 7D, Canon Inc., Japan) was used, with identical experimental parameters in each scenario. The camera and the lights were positioned far enough from the doorway so as not to interfere with the door and passage induced flows. Still images of the recorded videos are shown and discussed.

2.2.2. Experimental parameters

In the visualizations the ventilation rate in both rooms was set to 12 ACH so that the isolation room was in ~20 Pa negative pressure compared to the anteroom. Negative pressure was created by an imbalance between the supply and exhaust flow rates. However, the pressure difference between the rooms disappears when the doorway is open, leaving only the supply-exhaust flow rate differential effective between the rooms. This imbalance (between the anteroom and the isolation room) induces a net flow through the open doorway towards the isolation room (see Fig. 4 for illustration of the concept). Hence, it was decided to characterize the experimental conditions in terms of the supply-exhaust flow rate differential between the rooms, rather than using the pressure difference which is not effective during the door opening. A ~20 L/s flow rate difference between the rooms was measured during the door operation (resulting in ~20 Pa pressure difference between the rooms while doors were closed). The temperature difference between the rooms was small, making the thermally driven flows relatively weak.

2.3. Tracer gas measurements

2.3.1. Experimental methods

Tracer gas measurements were carried out to quantify the total

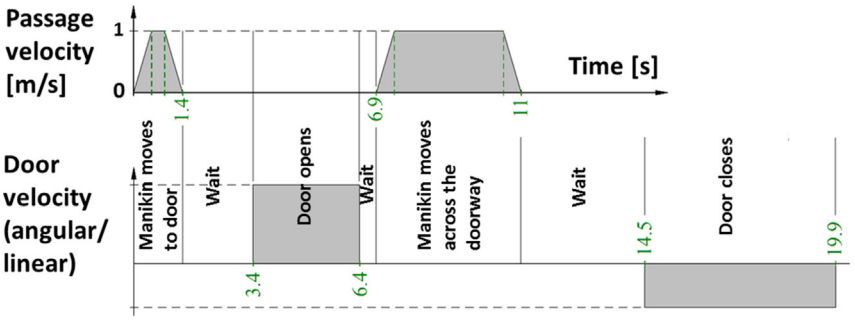

Fig. 3. Door operation and manikin movement (when applied) cycle for hinged and sliding doors.

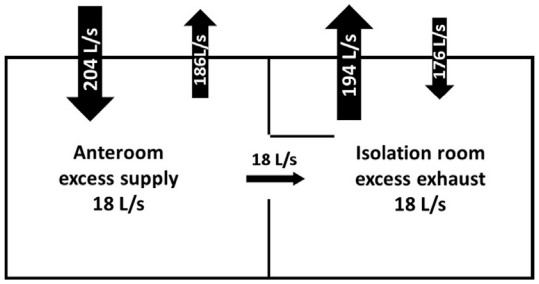

Fig. 4. Example of the supply-exhaust flow rate differentials and the induced net flow through the open doorway.

volume of air transferred through the doorway induced by the door operation. Two tracer gases, SF_6 and N_2O, were used simultaneously in the experiments. This made it possible to study the airflows through the doorway in both directions at once. The gases were supplied continuously into different rooms via supply ducts. Mixing ventilation with high airflow rates ensured quick and uniform distribution of the gases inside the rooms.

Two gas analysers (Brüel&Kjær model 1302, Brüel&Kjær A/S, Denmark), one for SF_6 and one for N_2O, were used to sample the tracers from the exhaust ducts. Following the onset of the dosing, the tracer gases achieved equilibrium concentrations in their separate rooms. Prior to a door operation the analysers were set to record the equilibrium values in the supply rooms. A moment before the door was opened the analysers were changed to sample the tracer concentration changes in the opposite, empty rooms (i.e. tracer free before the door operation). Short sampling period (sampling interval ~40 s) enabled sufficient tracking of the concentration changes within the rooms.

During the door operation the tracer gases flowed across the open doorway leading to a sudden increase in their concentrations in the opposite rooms. After the door had closed the tracer migration ceased and the concentrations started to decrease towards the initial background values prior the door operation (see Fig. 5).

The data analysis of the tracer gas measurements was based on the assumption that the tracers exited the isolation room model only through the exhausts, i.e. there were no leakages. This was considered a valid assumption as the model was made out of carefully fitted cleanroom elements.

The air exchange through the doorway was calculated based on the tracer migration from the supply room through the doorway to

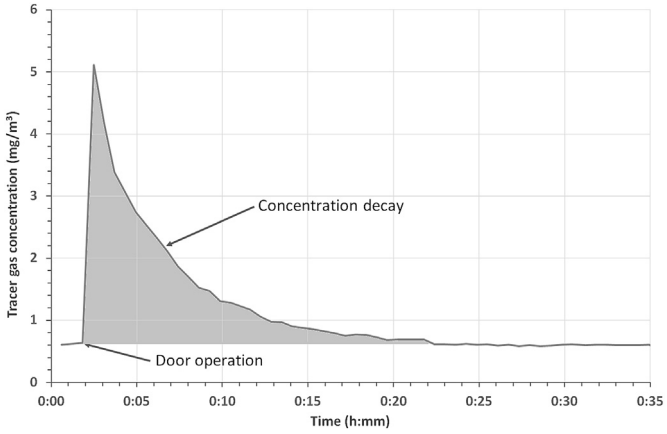

Fig. 5. Example of tracer gas concentration decay curve (measured from the exhaust duct).

the empty room induced by the door operation:

$$m_t = \rho_0 V \Rightarrow V = \frac{m_t}{\rho_0}, \tag{1}$$

where m_t is the total mass of the tracer gas migrating from the supply room to the empty room, ρ_0 is the initial concentration of the tracer gas in the release room and V is the volume migrating across the doorway to the empty room. After the door had closed the tracer migration ended and the concentration started to decrease (see Fig. 5). Since all the tracer gas leaves the room through the exhaust, the total amount of tracer can be calculated by integrating the exhaust concentration over time as:

$$m_t = Q_E \cdot \int_0^\infty \rho(t)dt, \tag{2}$$

where Q_E is the exhaust flow rate and $\rho(t)$ the measured tracer concentration in the exhaust. Substituting Equation (2) in (1) we get the total volume exchange across the doorway from the release room to the adjacent room induced by the door operation.

$$V = Q_E \cdot \int_0^\infty \frac{\rho(t)}{\rho_0} dt \approx Q_E \sum_i \frac{\rho_i}{\rho_0} \Delta t_i, \tag{3}$$

where, ρ_i is the ith tracer concentration measurement after the door operation and Δt_i is the sampling period of the ith measurement.

Typically, one experiment consisted of 6 door openings, each separated by 60 min. After each experiment the rooms were evacuated of the tracers, new experimental setup prepared and subsequently measurements carried out with it.

2.3.2. Experimental parameters

First the air volume migration induced by the door opening was measured with 0, 6 and 12 ACH ventilation rates (the anteroom and the isolation room having equal ACHs and 0 L/s supply-exhaust flow rate differential). Then ~20 L/s flow rate differential was added and the air exchange across the doorway measured with it (for both 6 and 12 ACH ventilation rates). Finally the manikin movement was added and the effect of passage and its direction was examined (under 6 and 12 ACH with ~20 L/s flow rate differential). The related baseline measurements without ventilation (i.e. 0 ACH) were reported earlier by Kalliomäki et al. [20].

3. Results

3.1. Smoke visualizations

Still images of the smoke visualization videos are shown in Figs. 6–11. Each figure has 6 panels (a-f), illustrating the smoke flow patterns during different phases of the door and passage cycles. Panel a shows the initial situation before the door is opened. Panel b shows the door opening-induced airflow patterns. Panel c depicts the combined effect of the door and the moving manikin. Panel d illustrates the situation just after the manikin has stopped. Panel e shows the flow patterns generated by the closing door and Panel f the mixing and dilution ~7 s after the door has been closed.

Fig. 6 shows the anteroom (i.e. Room 1 in Fig. 1) side-view of the single hinged door-generated airflow patterns. Fig. 6b shows that the door motion induces significant airflow through the doorway. Fig. 6c illustrates that the door-generated flow severely masks the wake behind the moving manikin. However, Fig. 6d shows that a notable amount of air is dragged in the wake which can be seen

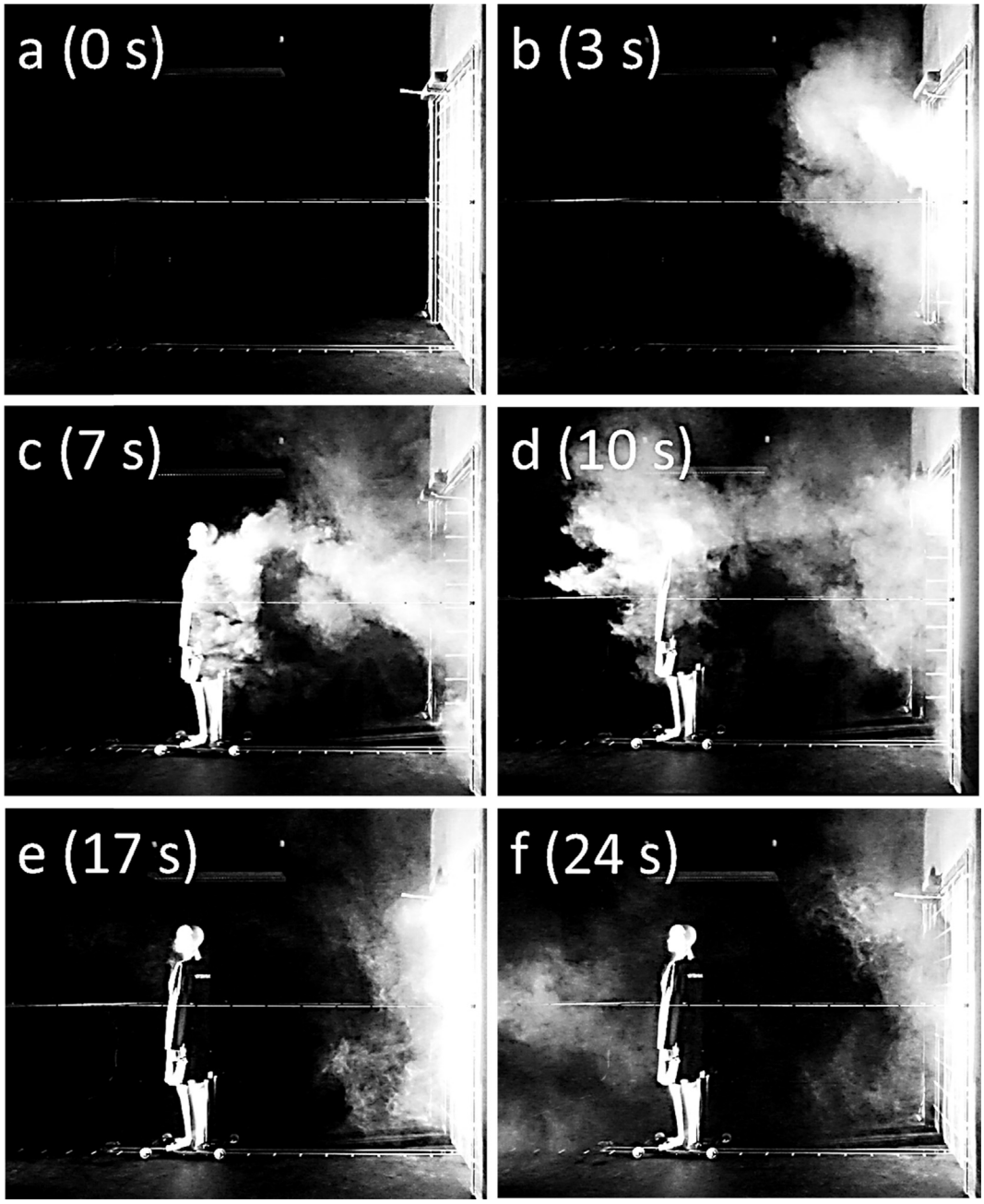

Fig. 6. Smoke visualization (anteroom side-view) of the single hinged door and manikin passage induced airflow patterns with 12 ACH ventilation rate and 18 L/s flow rate differential. The time in the parenthesis denotes the time elapsed since the door started opening.

moving past the now stationary manikin. The door motion does not seem to cause any significant air movements in the anteroom while closing (Fig. 6e). The smoke is spread and mixed (partly vanishing from the lit section) due to effective ventilation (Fig. 6f).

Fig. 7 shows the anteroom top-view of the single hinged door-induced airflow patterns. Fig. 7b shows that the smoke penetrates far into the room. From this viewpoint, the wake behind the manikin is masked by the door motion-induced airflow (Fig. 7c). However, Fig. 7d shows that a notable amount of air is carried in the wake and can be seen to move past the now stationary manikin. The door motion does not seem to cause any significant airflows while closing (Fig. 7e). Again, the smoke is spread inside the room due to ventilation and partly vanishes from the lit section (Fig. 7f).

Fig. 8 shows the isolation room (i.e. Room 2 in Fig. 1) side-view of the single hinged door-induced airflow patterns. The sweeping door drags notable amount of the anteroom air into the isolation room (Fig. 8b). Fig. 8c shows that the wake is coupled with the door-induced flow and difficult to distinguish. Nevertheless, in Fig. 8d a significant amount of smoke can be seen to flow past the stopped manikin. The sweeping door seems to induce air movement by pushing the air towards the viewer while closing (Fig. 8e). After the door has closed the smoke disperses into the room and is mixed throughout the room partly vanishing from the lit section (Fig. 8f).

Fig. 9 shows the isolation room top-view of the single hinged door-generated airflow patterns. Fig. 9b shows that the sweeping door forms a vortex. The effect of the moving manikin cannot be distinguished from the door motion induced flow (Fig. 9c). However, after the manikin has stopped some of the air can be seen

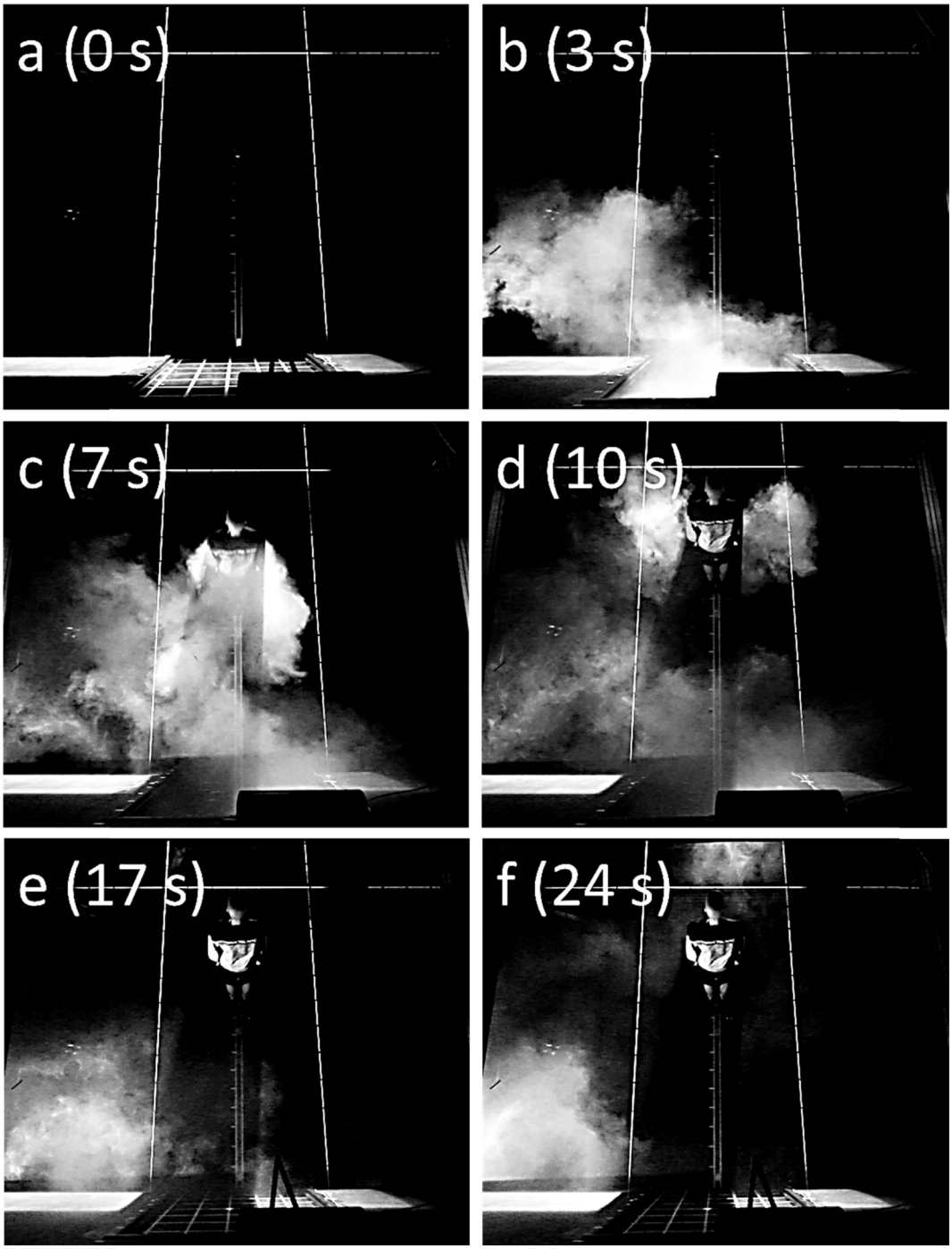

Fig. 7. Smoke visualization (anteroom top-view) of the single hinged door and manikin passage induced airflow patterns with 12 ACH ventilation rate and 18 L/s flow rate differential. The time in the parenthesis denotes the time elapsed since the door started opening.

flowing past it (Fig. 9d). The closing door pushes the air towards the right corner of the room (Fig. 9e). Fig. 9f shows that the air is spread around the room (and partly disappears from the lit section).

Fig. 10 shows the anteroom side-view of the sliding door-generated airflow patterns. The door-opening induces only modest flow through the doorway (Fig. 10b). The wake behind the moving manikin can now be seen clearly (Fig. 10c). The manikin drags significant amount of air with it to the anteroom, which can be seen flowing past it after it has stopped (Fig. 10d). The sliding door does not seem to generate any notable air movements across the doorway while closing (Fig. 10e). The smoke is quickly mixed across the room partly vanishing from the lit section (Fig. 10f).

Fig. 11 shows the anteroom top-view of the sliding door-generated airflow patterns. Fig. 11b shows that the induced airflow is modest also in horizontal direction. The wake behind the moving manikin can be seen clearly (Fig. 11c). The manikin drags substantial amount of air with it to the anteroom (Fig. 11d). The door motion does not generate notable air movements in the doorway while closing (Fig. 11e). The air is spread around the room partly disappearing from the lit section as seen from Fig. 11f. Only anteroom visualizations for the sliding door are shown as the flow patterns were essentially similar on both sides of the doorway.

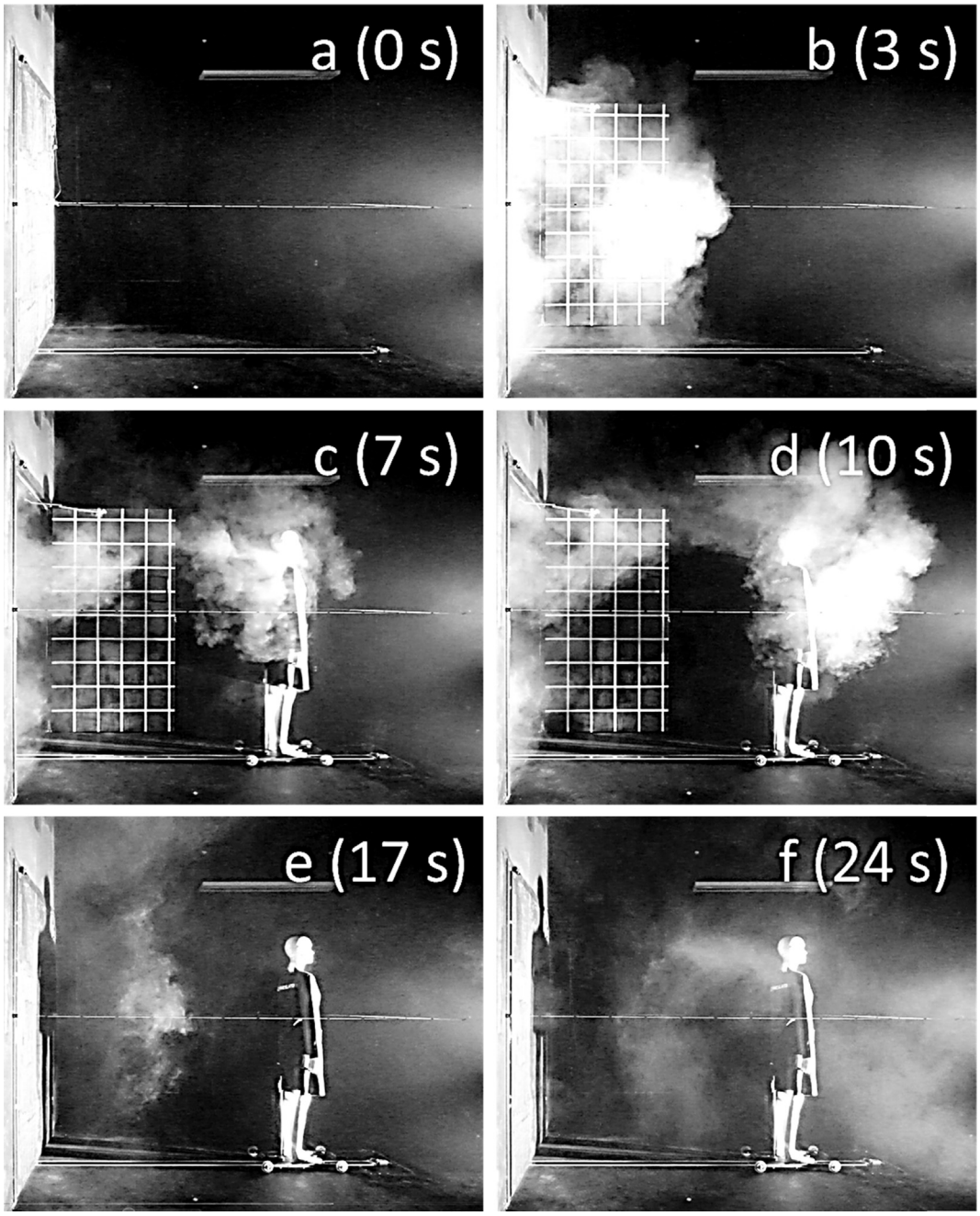

Fig. 8. Smoke visualization (isolation room side-view) of the single hinged door and manikin passage induced airflow patterns with 12 ACH ventilation rate and 18 L/s flow rate differential. The time in the parenthesis denotes the time elapsed since the door started opening.

3.2. Tracer gas measurements

The tracer gas measurement results are shown in Table 1 and illustrated in Figs. 12–15. The main focus is on the air volume escaping the isolation room (i.e. from Room 2 to Room 1, marked with 2 → 1 in Table 1) induced by the door operation as it was considered more important than the air volume entering the isolation room regarding the breakdown of isolation conditions. However, few baseline results are shown for both flow directions for illustration of the two-way exchange. The uncertainty of the results is estimated by standard deviation for each examined case. In the last column of Table 1 the results are shown normalized relative to the swept volume of the hinged door.

3.2.1. Ventilation rate

The effect of different ventilation rates (i.e. 0, 6 and 12 ACH with ~0 L/s flow rate differential) is shown in the first subsection of Table 1 and illustrated in Fig. 12. In this case the experiments were performed without passage. The results show that there was a notable difference in the air exchange volume through the doorway between the hinged and sliding doors. The sliding door motion induced significantly weaker air exchange across the doorway than the hinged door. The air exchange volume was found to be similar to both directions across the doorway with both door types.

The effect of ventilation rate seemed to be rather small with the hinged door. Only a slight increase in the induced air exchange across the doorway was observed with increasing ventilation rates,

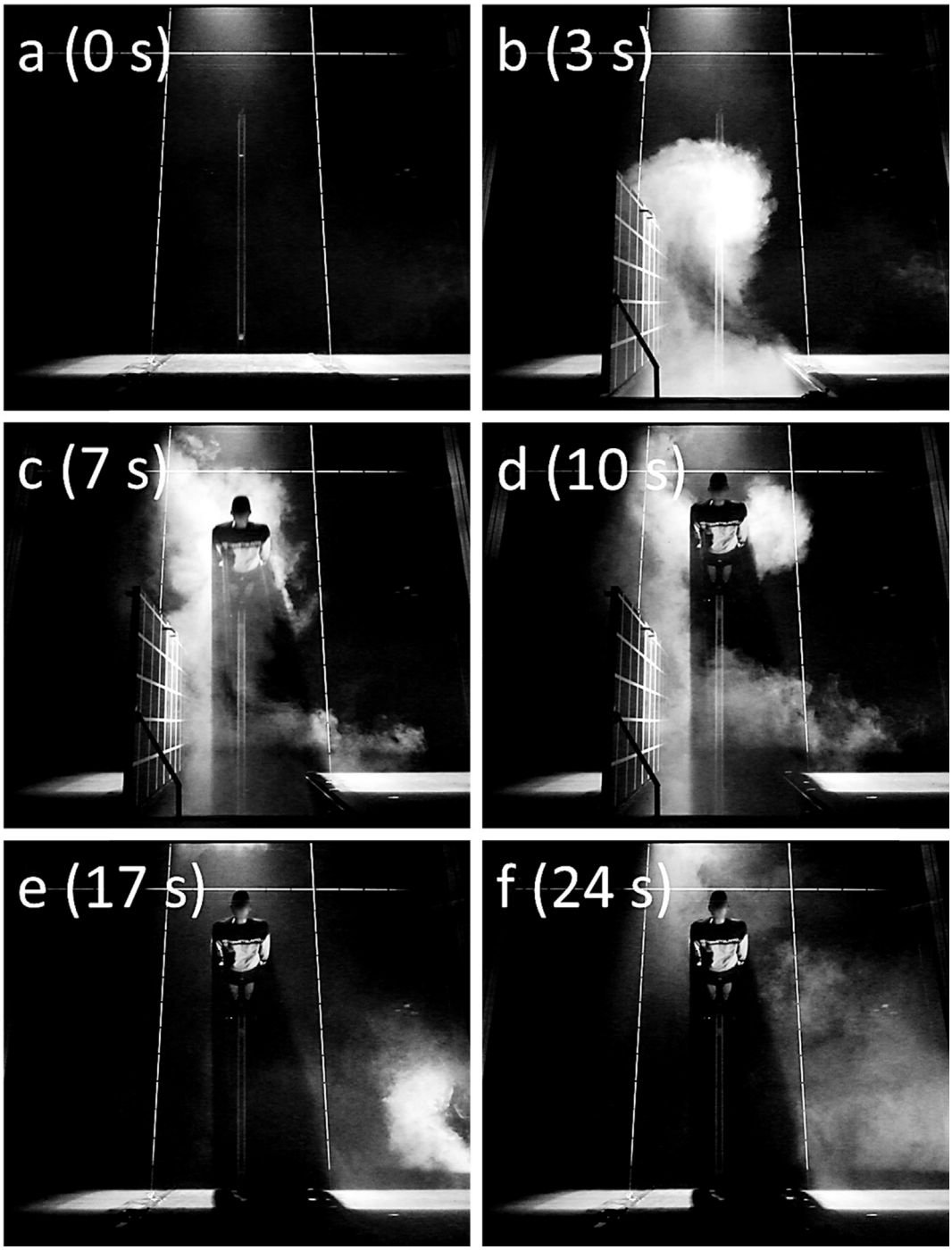

Fig. 9. Smoke visualization (isolation room top-view) of the single hinged and manikin passage induced airflow patterns with 12 ACH ventilation rate and 18 L/s flow rate differential. The time in the parenthesis denotes the time elapsed since the door started opening.

the results being almost the same with 6 and 12 ACH. However, the impact with sliding door was more notable. The 6 ACH decreased the air volume transfer slightly compared to the baseline scenario without ventilation (i.e. 0 ACH). The effect seemed to be opposite for the 12 ACH case as the air exchange volume increased notably compared to 6 ACH case.

3.2.2. Flow rate differential (pressure difference)

The effect of supply-exhaust flow rate differential (i.e. net flow towards isolation room across the open doorway) with 6 ACH and 12 ACH ventilation rates is presented in the second subsection of Table 1 and illustrated in Fig. 13. The measurements were performed without passage in this case as well. The results show that the flow differential reduced the door motion-generated air transfer out of the isolation room with both door types and with both ventilation rates. Relative reduction was greater with sliding door (with both ventilation rates).

3.2.3. Passage and its direction

The effect of passage and its direction with 6 and 12 ACH (both

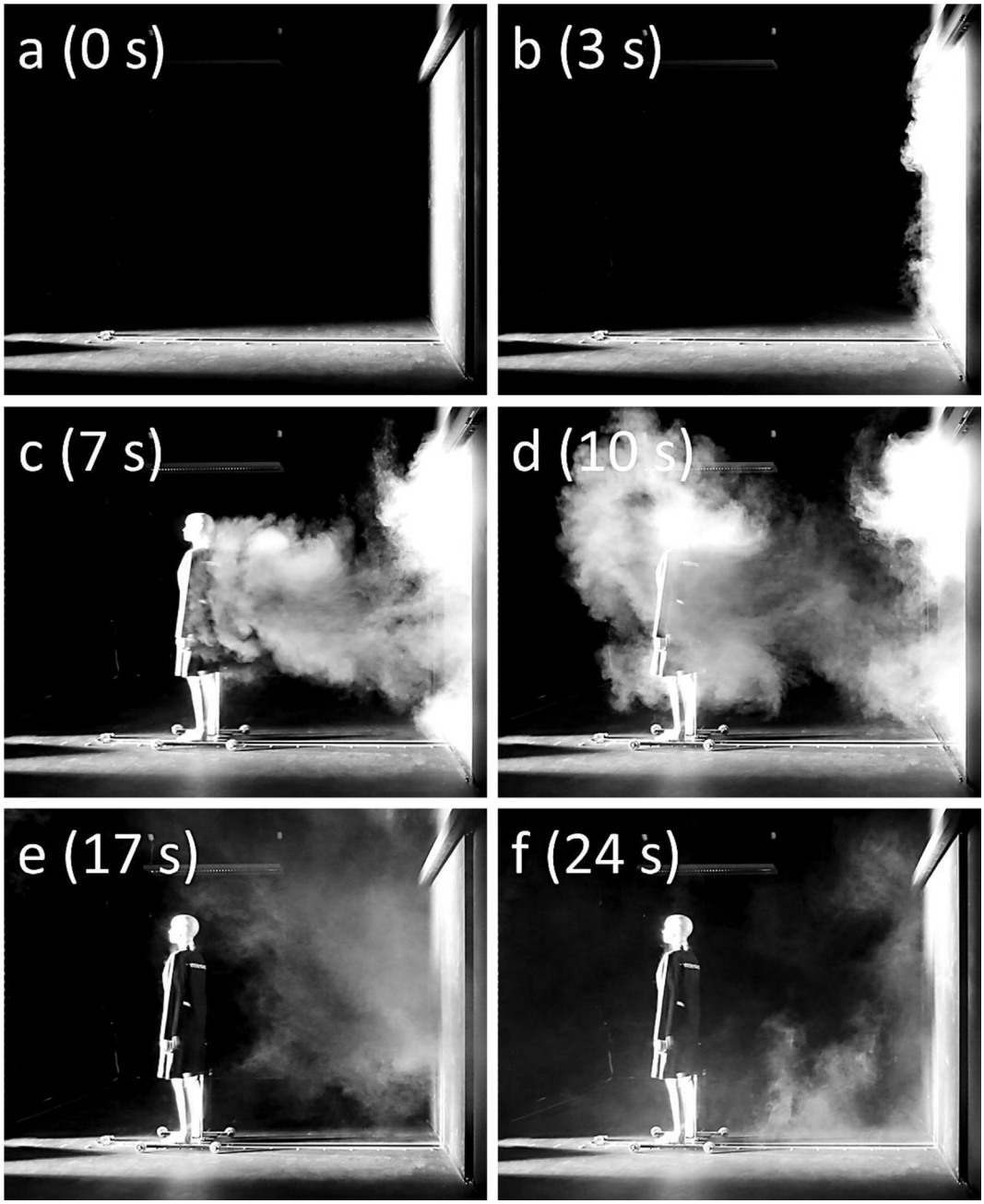

Fig. 10. Smoke visualization (anteroom side-view) of the single sliding door and manikin passage induced airflow patterns with 12 ACH ventilation rate and 20 L/s flow rate differential. The time in the parenthesis denotes the time elapsed since the door started opening.

with ~20 L/s flow rate differential) is shown in the last subsection of Table 1 and illustrated in Figs. 14 and 15. The effect of passage seemed to be notable with both door types and with both ventilation rates. The airflow out of the isolation room appeared to be almost independent of the passage direction (entry/exit). Only with 6 ACH the exit through the hinged door seemed to generate greater total volume transfer compared to entry.

4. Discussion

4.1. Flow visualizations

Although smoke has been used long and widely in fluid flow visualizations [40] there seems to be no report on experimental full-scale smoke visualizations comparing hinged and sliding door motion-induced airflow patterns performed using realistic isolation room ventilation rates.

In a baseline study carried out by Tang et al. [19] the hinged and sliding door motion-induced doorway flows were qualitatively visualized using colored food dye in a small-scale water model without ventilation imposed. In another closely linked baseline study Kalliomäki et al. [20] examined the single hinged and sliding doors induced airflow patterns in an identical full-scale isolation room model also without ventilation imposed. Compared against these baseline studies the general qualitative flow patterns with ventilation were found to be similar: the hinged door generated more pronounced flow across the doorway than the sliding door, passage was found to increase the airflow through the doorway,

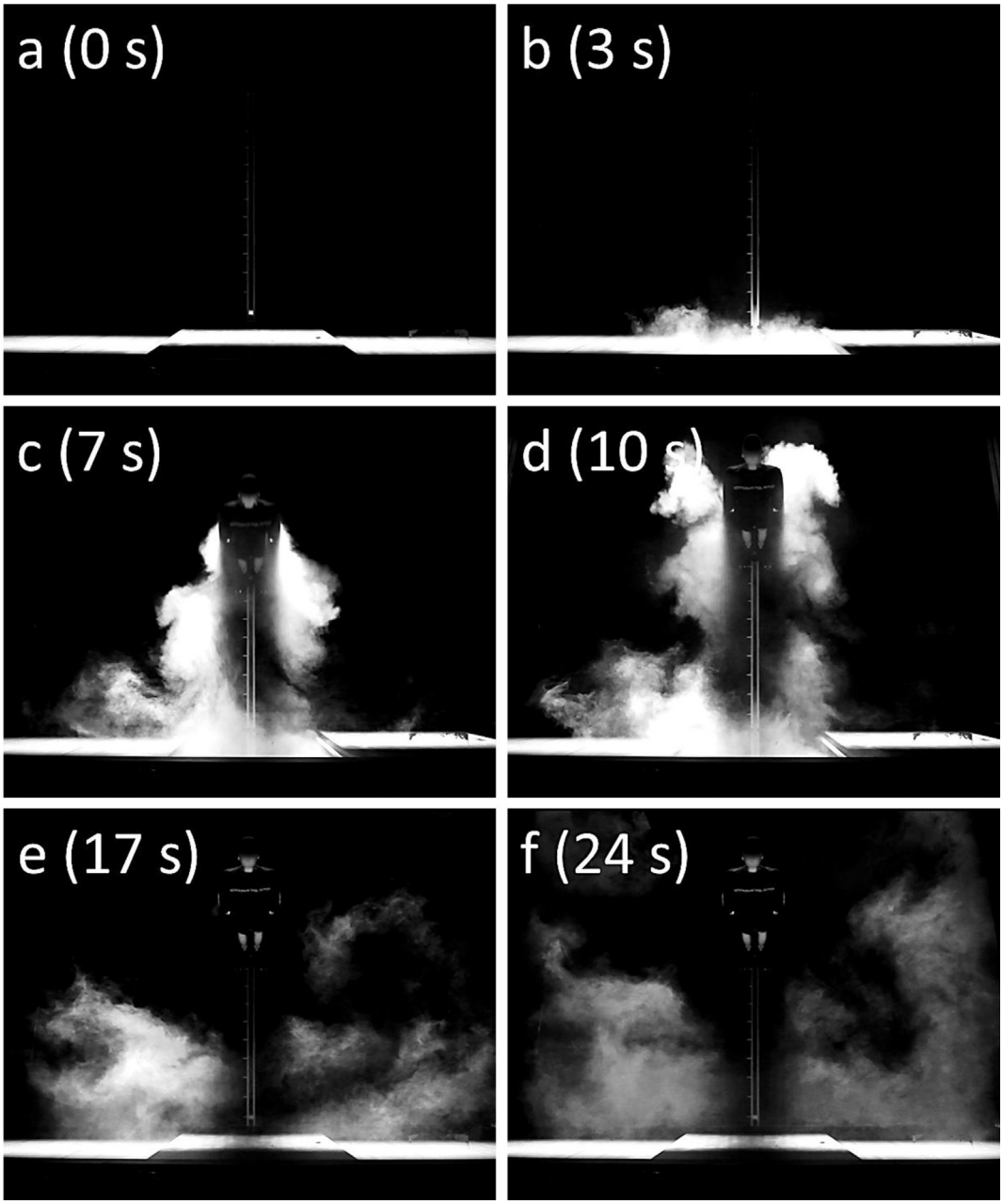

Fig. 11. Smoke visualization (anteroom top-view) of the single sliding door and manikin passage induced airflow patterns with 12 ACH ventilation rate and 20 L/s flow rate differential. The time in the parenthesis denotes the time elapsed since the door started opening.

door vortex formed behind the sweeping hinged door etc. On the other hand, comparison also shows that there are some differences in the flow structures. For example, ventilation appeared to effectively mix and dilute the smoke throughout the room. Hence the flow structures (door vortices, wake of the manikin etc.) were seen somewhat unclear and they vanished quicker from the lit section. Nevertheless, based on the qualitative assessment of the smoke visualizations alone, it is difficult to distinguish whether the ventilation or flow rate differential used in the experiments increased or reduced the flow through the doorway.

Most of the other studies have visualized the door operation generated flows e.g. with small-scale water models using different dyes as tracers [19,22,24] or with CFD approaches in various scenarios using several different boundary conditions and methods [23,26,31,32,34]. Nevertheless, they all concluded that opening of the hinged door can generate notable flow through the doorway and hence disperse airborne contaminants across the doorway. This phenomenon was also observed and verified in the full-scale experiments reported here. However, common to above mentioned studies is that they lack experimental visualizations for the sliding door option, which makes the visualizations presented here unique.

4.2. Tracer gas measurements

4.2.1. The effect of ventilation rates

The smoke visualizations are only qualitative in nature and based on them one cannot measure the air volume exchange across the doorway induced by the door operation. Hence we carried out tracer gas measurements to define this quantitatively. The results

Table 1
Results of the tracer gas measurements.

Door type	Door cycle time (open/hold/close)	Air change rate[a] (ACH)	Flow diff.[b] (L/s) (Pa[c])	Passage	Avg. air volume exchange (m^3) 1 → 2	Avg. air volume exchange (m^3) 2 → 1	Standard deviation (m^3) 2 → 1	Normalized air volume exchange[d] 2 → 1
With different air changes per hour:								
Hinged	3/8/5.4 s	0	0 (0)	–	1.30	**1.39**	0.12	0.69
Sliding	3/8/5.4 s	0	0 (0)	–	0.54	**0.56**	0.07	0.28
Hinged	3/8/5.4 s	6.1	c. 0 (0)	–	1.32	**1.45**	0.13	0.72
Sliding	3/8/5.4 s	6.1	c. 0 (0)	–	–	**0.42**	0.07	0.21
Hinged	3/8/5.4 s	12.2	c. 0 (0)	–	1.54	**1.47**	0.12	0.73
Sliding	3/8/5.4 s	12.4	c. 0 (0)	–	0.76	**0.84**	0.20	0.42
With pressure difference:								
Hinged	3/8/5.4 s	6.1	25 (−21)	–	–	**1.17**	0.17	0.58
Sliding	3/8/5.4 s	6.0	25 (−21)	–	–	**0.27**	0.09	0.13
Hinged	3/8/5.4 s	12.0	18 (−21)	–	–	**1.31**	0.22	0.66
Sliding	3/8/5.4 s	12.2	21 (−21)	–	–	**0.54**	0.17	0.27
With passage:								
Hinged	3/8/5.4 s	6.0	22 (−21)	Both dir.	–	**1.51**	0.16	0.75
Sliding	3/8/5.4 s	6.1	24 (−21)	Both dir.	–	**0.50**	0.06	0.25
Hinged	3/8/5.4 s	6.0	23 (−21)	2 → 1	–	**1.62**	0.05	0.81
Sliding	3/8/5.4 s	6.1	24 (−21)	2 → 1	–	**0.49**	0.09	0.25
Hinged	3/8/5.4 s	6.0	21 (−21)	1 → 2	–	**1.34**	0.05	0.67
Sliding	3/8/5.4 s	6.1	25 (−20)	1 → 2	–	**0.50**	0.04	0.25
Hinged	3/8/5.4 s	12.0	18 (−21)	Both dir.	–	**1.56**	0.21	0.78
Sliding	3/8/5.4 s	12.2	20 (−22)	Both dir.	–	**0.78**	0.14	0.39
Hinged	3/8/5.4 s	12.0	18 (−21)	2 → 1	–	**1.58**	0.26	0.79
Sliding	3/8/5.4 s	12.2	21 (−22)	2 → 1	–	**0.82**	0.20	0.41
Hinged	3/8/5.4 s	12.0	18 (−21)	1 → 2	–	**1.54**	0.18	0.77
Sliding	3/8/5.4 s	12.2	19 (−22)	1 → 2	–	**0.73**	0.07	0.36

[a] Measured from the isolation room exhaust (both rooms had the same ventilation rates).
[b] Flow rate differential (supply − exhaust) between rooms while door open.
[c] Pressure difference between the rooms before door opening (isolation room in lower pressure).
[d] Normalized by the swept volume of the hinged door ($1/4 \times \pi \times w^2_{door} \times h_{door}$).

show that the examined ventilation rates do not affect notably the air volume migration out of the isolation room during hinged door operation. In principle, increasing ventilation rates can generate more turbulence which in turn can enhance the mixing across the open doorway [41]. However, it should be noted that in general, increased ventilation rates improve the containment as the concentration of particles and gaseous agents are more quickly diluted already in an isolation room [21,38]. Hence, less agents are dispersed from an isolation room into an anteroom and subsequently less of a fraction can enter other neighboring spaces [21].

Saarinen et al. [42] showed that the hinged door opening motion itself can generate velocities over 1.0 m/s in the doorway. Also the smoke visualizations shown here illustrate that the opening induce fast and swirling flow across the doorway. High momentum supply air can generate high air velocities in the room and around the doorway as well. In the experiments, however, the section of the supply air terminal towards the doorway was blocked and thus the air movements caused by the supply air jet were assumed to be only modest close to the door. Hence it seems like the hinged door motion itself creates strong mixing which dominates or at least delays the onset of the ventilation generated effects in the doorway (with the examined ventilation rates at least).

The sliding door motion induced airflow seemed to be rather modest and hence the air velocities (and turbulence) in the doorway might be dominated by the ventilation flows. Thus the

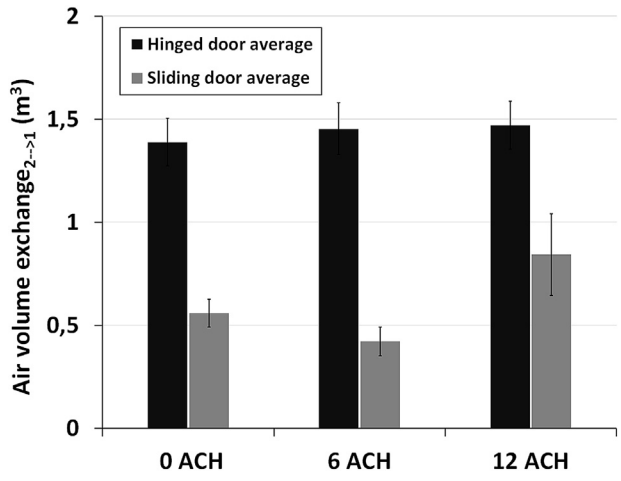

Fig. 12. Tracer gas measurement results. The effect of ventilation rate on the air volume transfer across the doorway (with 0 L/s flow rate differential).

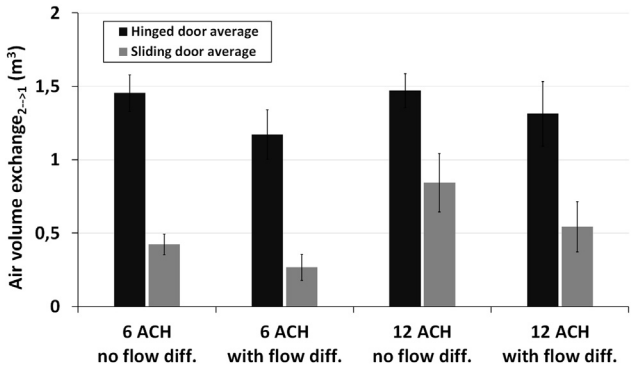

Fig. 13. Tracer gas measurement results. The effect of supply-exhaust flow rate differential on the air volume transfer across the doorway.

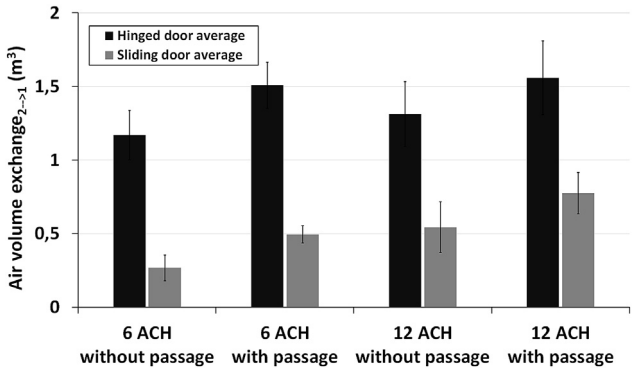

Fig. 14. Tracer gas measurement results. The effect of manikin passage on the air volume transfer across the doorway.

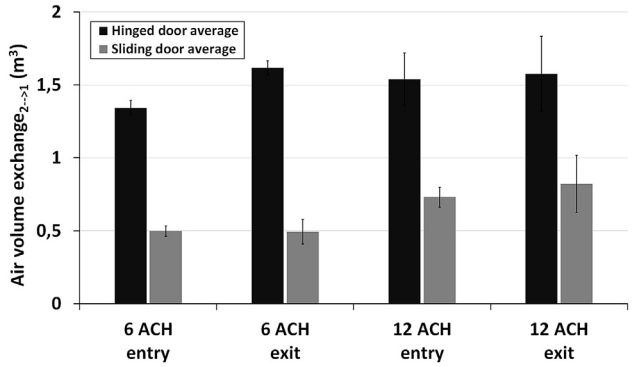

Fig. 15. Tracer gas measurement results. The effect of passage direction on the air volume transfer across the doorway.

onset of the ventilation generated mixing across the doorway is not severely delayed by the sliding door opening motion and hence can result in increased air exchange through the doorway (seen well with 12 ACH in this study). However, this should be confirmed in the future with additional measurements with complementary ventilation rates.

4.2.2. The effect of supply-exhaust flow rate differential

The supply-exhaust flow rate differential was observed to reduce the door opening induced air exchange across the doorway with both door types and ventilation rates (see Fig. 13). However, it is not yet precisely clear how effective it is in reducing the air from escaping an isolation room as it has been more in common to examine the effect of pressure difference although it vanishes when the door is opened. For instance, Adams et al. [28] and Mousavi and Grosskopf [32] have pointed out that pressure difference significantly reduces the aerosol transfer through the doorway during hinged door operation. However, only few have estimated or measured the effect of flow rate differentials for both hinged and sliding doors. For instance, Shaw [17] found that 0.30 m^3/s excess flow for sliding door (with 1 °C temperature difference across the doorway) would be needed to reduce the transfer close to zero (however, no data were reported for hinged door). Later, Hayden et al. [18] observed that flow rate differential was the only parameter (of the examined variables) significantly affecting the air volume migration through the isolation room doorway generated by hinged and sliding doors. They estimated that flow rate differential of c. 0.36 m^3/s (c. 0.26 m^3/s) would be enough to decrease the air transfer through the doorway to close to zero during hinged (sliding) door operation.

According to the data presented in the first and second subsection of Table 1 it can be estimated (by linear regression) that 0.13 m^3/s and 0.06 m^3/s supply-exhaust flow rate differential (net flow towards isolation room) for hinged and sliding doors (respectively) are required to reduce the escaping air to zero. However, one should note that in practice the door motion-induced flow can penetrate far into the rooms (especially with hinged door) and might not be directed back through the doorway (while open) but will stay in the room. Besides, maintaining high flow rate differentials constantly requires controlled leakage and elevated ventilation rates and thus is not energy efficient. More practical solutions should be considered instead. One solution would be to increase the flow rate differential temporarily during door operation only. Kim and Augenbroe [43] suggested realizing this by adaptive VAV (variable air volume) method normally keeping a low flow rate differential but capable of increasing it to higher values prior and during door operation. This kind of method sounds promising but more detailed studies are required to define how feasible these kinds of applications are in a real hospital environment.

4.2.3. The effect of simulated human passage

The effect of passage is also important since it increases the airflow through the isolation room doorway during door operation. Although moving body induced airflows and dynamics of wake flow field in different types of indoor environments (isolation rooms, offices, air planes etc.) have been studied extensively [12–16,24,44–51] not many have quantified the passage generated air volume exchange through a doorway. It is important to know how much passage contributes to the air transfer between spaces with different door solutions. It might well be that the door type does not matter if passage is the main contributor to transient breakdown of the isolation conditions related to door operation.

Hayden et al. [18] examined the effect of a moving manikin on the air volume migration induced by hinged and sliding doors in a full-scale isolation room model. They estimated the effect of passage to be 0.34 m^3 with the hinged door and 0.81 m^3 with the sliding door on average. Surprisingly high air volume migration generated by the passage through the sliding door lead to conclusion that both door types performed equally well.

However, this seems not to be the case in here as can be seen from the last subsection of Table 1. It shows that the passage alone induces 0.25 m^3–0.34 m^3 (6–12 ACH) air volume transfer through the doorway with the hinged door and 0.23 m^3–0.24 m^3 with the sliding door (averaged over both directions, the effect of passage direction will be discussed later).

In a related baseline study Kalliomäki et al. [20] examined the airflow patterns across the isolation room doorway in an identical full-scale model without ventilation. They found the effect of the manikin passage to be 0.27 m^3 and 0.36 m^3 on average with the hinged and sliding doors respectively. These results agree well with the ones presented in this study. These results imply that the effect of passage is not as large for the sliding door as suggested by Hayden et al. [18]. Hence the sliding door performs much better than the hinged door, even when combined with passage.

Passage direction might also affect the doorway flows. In the closely related baseline study performed without ventilation, Kalliomäki et al. [20] found out that moving against the opening direction of the single hinged door, the passage amplified the doorway flows resulting in a higher air volume transfer across the doorway compared to the other passage direction. However, Hayden et al. [18] and Kokkonen et al. [25] did not find any significant effect of the passage direction on the air volume migration across the isolation room doorway when realistic ventilation rates were used. Fig. 14 shows that for the hinged door the exit seems to

generate greater air volume migration than entry with 6 ACH. However, with 12 ACH the induced air exchange appeared to be independent of the passage direction. Hence it seems like airflows generated by the 12 ACH ventilation rate are strong enough to cancel the effect of passage direction. With the sliding door this appeared to be insignificant with both ventilation rates. Thus it seems that at least high ventilation rates can mask the effect of moving direction.

4.3. Normalized results

For easier comparison with other previous studies the normalized results (with respect to swept volume of the hinged door) are shown in the last column of Table 1. The normalized air exchange seems to vary between 58–81% for hinged door and between 13–42% for sliding door depending on the tested scenario. The hinged door results agree reasonably well with findings reported in previous studies. For instance, Eames et al. [29] reported the exchange volume to be comparable to but less than swept volume of the hinged door. On the other hand, Kiel and Wilson [54] found out the typical exchange volume (for hinged door) to be only around 50% of the swept volume. Kalliomäki et al. [20] measured the exchange volume (for hinged door) to be 59–124% and Hathway et al. [22] measured it to be 67–98% of the swept volume of the hinged door. However, one should note that most of the above mentioned studies were carried out in scale models with different door cycle times and/or without ventilation. So, one should be cautious while directly comparing the results. Comparison of sliding door results is more challenging since there are no other normalized (experimental) results readily available.

4.4. Limitations of using a manikin, set door open-close cycle time and isothermal conditions

One might argue that a manikin might not simulate realistically the formation of a human movement induced flow field which is very complex, dynamic and turbulent mixing process [15,47–50]. For instance, basic plastic manikin used in this study does not take into account legs or arms movement. However, as found out by Han et al. [49], the body motion has a greater effect on the induced airflows and aerodynamics than that of limbs pendulum. Also, Moyer et al. [51] have assessed that swinging of arms has little significance in the formation of the wake. Finally and most convincingly, Shaw [17], who is one of the few who has measured the amount of air dragged behind a real person moving between a treatment room and an associated lobby in a hospital setting, found the effect of passage to be 0.29 m^3 during fast walk. The manikin induced air exchange reported here agrees quite well with this value and, in this regard, can simulate the human passage fairly realistically.

The manikin used in this study was not heated. The lack of human thermal plume could in principle affect the airflow patterns. However, based on the results obtained by Wu and Gao [16] the wake flow dominates over the thermal flows induced by the body heat when moving faster than 0.4 m/s. Also, Licina et al. [52] found out that horizontal flow of 0.425 m/s towards a manikin completely replaced the upward convective boundary layer flow with air flows parallel to horizontal flow. Hence, the effect of thermal plume of the body can be assumed to be negligible in this case.

In reality there are other heat loads, besides the manikin, in isolation rooms such as lights, monitoring equipment, solar load, patient etc. These heat loads can heat up the rooms and generate temperature difference between an isolation room and an anteroom or a corridor. Already a small temperature difference induces continuous two-way air exchange across open doorway substantially increasing the total air volume migration during door operation [21,53]. This effect becomes increasingly important when door is kept open long periods [20–22]. However, we decided to carry out the experiments without any heat loads and close to isothermal conditions as it would have been very challenging or even impossible to monitor and control small temperature differences (~0–0.5 °C) potentially present between isolation rooms and anterooms [17,21]. Besides, small temperature differences cannot be excluded as the accuracy of the thermometers used in this study was ±0.2 °C. Nevertheless, applying realistic temperature differences might increase slightly the air exchange volumes reported here.

The total cycle time of the door used in this study can be considered slightly too long compared to typical scenarios in critical hospital environments (like in isolation rooms). Shaw [17] examined the door opening habits (of manual or semi-manual doors with self-closers) in seven isolation rooms in six different hospitals and found the average total cycle time of the door to be between 7 and 10 s. However, the cycle time with automated doors can be longer as typically they open completely whereas with manually operated doors people tend to sneak in through only partly opened door. Moreover, the door operation cycle in this study was set loose enough to avoid collision of the manikin and the door. Nevertheless, using shorter cycle time can probably lead to reduced air exchange across the doorway as found out by Kalliomäki et al. [20] and Hathway et al. [22].

4.5. Use of anterooms

One way to prevent the isolation room air from escaping directly to corridor is using an anteroom between the spaces. Anteroom captures, dilutes and exhausts most of the contaminants escaping the isolation room through the doorway, thus serving as an effective isolation barrier between the dirty and clean zones. As with isolation rooms, containment efficiency of anterooms can be increased with higher ventilation rates as then the airborne contaminants are diluted even quicker and hence less agents can escape to adjacent spaces [21].

In this study the anteroom and isolation rooms were equal in size. However, in practice the anteroom is typically smaller than the isolation room. There seems to be no clear consensus how the room sizes affect the door motion-induced flows and air volume migration through the doorway though. Hayden et al. [18] suggested that a small anteroom might reduce and a large one increase the air volume migration to corridor. On the other hand, Kiel and Wilson [54] found out that the air exchange across the outer door of a small test house was not notably influenced by the room size or layout. However, more detailed studies are needed in order to define the effect of room size explicitly. Nevertheless, the anteroom should be utilized correctly to fulfill its contaminant dispersion prevention potential. For example, the doors should always be interlocked so that only one of the doors can be open at a time. Also, the anteroom should not be shared with another isolation room or rooms. Hang et al. [21] have shown that a shared anteroom can lead to contaminant transport between isolation rooms due to a hinged door opening motion. Hence, non-shared anterooms should be preferable.

5. Conclusions

It has been shown explicitly in this study that a single sliding door operation induces less airflow across the isolation room doorway and hence performs substantially better than a single hinged door in various realistic operation scenarios.

The smoke visualizations showed that door motion was capable

of inducing air exchange across the doorway with both door types. However, the hinged door motion-generated airflow was more pronounced compared to the sliding door. Also the effect of passage was notable. The manikin carried significant amount of air in its wake through the doorway. The effect of passage was clearer with the sliding door, as its contribution to the doorway exchange flows was relatively large by comparison. Ventilation was seen to affect the generated flow patterns. It effectively mixed and diluted the smoke and hence the flow structures were slightly unclear and vanished quickly from the lit section of the rooms. However, from the smoke experiments alone it was difficult to distinguish whether the ventilation increased or reduced the door motion-induced airflows.

Tracer gas measurements showed quantitatively that the door operation induced substantial air exchange through the doorway. The measured air volume exchange varied between 1.17–1.62 m^3 for the hinged door and between 0.27–0.84 m^3 for the sliding door on average (depending of the examined scenario). The examined ventilation rates (6 and 12 ACHs) were observed to have only a small effect on the air escaping the isolation room caused by the hinged door operation. For the sliding door the effect was seen to be more variable. The flow rate differential (~20 L/s net flow towards the isolation room when the door was open) was found to decrease the air volume migration across the doorway with both door types and ventilation rates. The reduction was observed to be greater with the sliding door (relative to the hinged door). Passage increased the air exchange through the doorway with 0.25–0.34 m^3 for the hinged door and 0.23–0.24 m^3 for the sliding door on average. In conclusion, the sliding door appeared to perform better in each studied scenario. Hence, it should be considered as a primary door type in isolation rooms.

In future, the door operation generated isolation room containment failures should be further explored with various realistic parameter settings (i.e. with realistic heat loads, additional flow rate differentials, and real human passage) for even better understanding of the factors related to door usage-induced airborne contaminant dispersal.

Acknowledgement

Funding for this study was provided by the Finnish Funding Agency for Technology and Innovation (TEKES, grant number 40301/10). It was part of a larger project co-funded by TEKES and A*STAR (Agency for Science, Technology and Research, Singapore, grant number 102 129 0099). Additionally the authors would like to thank Jarkko Hakala and David Oliva for their efforts and help when constructing the full-scale isolation room model.

References

[1] X. Xie, Y. Li, H. Sun, L. Liu, Exhaled droplets due to talking and coughing, J. R. Soc. Interface 6 (2009) S703–S714.
[2] L. Morawska, G.R. Johnson, Z.D. Ristovski, M. Hargreaves, K. Mengersen, S. Corbett, C.Y.H. Chao, Y. Li, D. Katoshevski, Size distribution and sites of origin of droplets expelled from the human respiratory tract during expiratory activities, J. Aerosol Sci. 40 (2009) 256–269.
[3] W.F. Wells, In air-borne infection. Study II. Droplets and droplet nuclei, Am. J. Hyg. 20 (1934) 611–618.
[4] X. Xie, Y. Li, A.T.Y. Chwang, P.L. Ho, W.H. Seto, How far droplets can move in indoor environments – revisiting the wells evaporation-falling curve, Indoor Air 17 (2007) 211–225.
[5] ASHRAE, HVAC Design Manual for Hospitals and Clinics, ISBN 1-931862-26-5, ASHRAE, Atlanta, GA, USA, 2013.
[6] FGI, Guidelines for Design and Construction of Hospitals and Outpatient Facilities, ASHE, Chicago, IL, 2014.
[7] CDC, Guidelines for Preventing the Transmission of Mycobacterium tuberculosis in Health-care Settings, vol. 54, MMWR, Washington, DC, 2005, 2005.
[8] Health Building Note 04-01, Adult In-patient Facilities, Department of Health, UK, 2013.
[9] J.W.-T. Tang, Y. Li, I. Eames, P.K.S. Chan, G.L. Ridgway, Factors involved in the aerosol transmission of infection and control of ventilation healthcare premises, J. Hosp. Infect. 64 (2006) 100–114.
[10] N. Pavelchak, R. DePersis, M. London, R. Stricof, M. Oxtoby, G. DiFerdinando, E. Marshall, Identification of factors that disrupt negative air pressurization of respiratory isolation rooms, Infect. Control Hosp. Epidemiol. 21 (2000) 191–195.
[11] J.W.-T. Tang, I. Eames, Y. Li, Y.A. Taha, P. Wilson, G. Bellingan, K.N. Ward, J. Breuer, Door-opening motion can potentially lead to a transient breakdown in negative-pressure isolation conditions : the importance of vorticity and buoyancy airflows, J. Hosp. Infect. 61 (2005) 283–286.
[12] S. Okamoto, Y. Sunabashiri, Vortex shedding from a circular cylinder of finite length placed on a ground plane, J. Fluids Eng. 114 (1992) 512–521.
[13] B.A. Edge, E.G. Paterson, G.S. Settles, Computational study of the wake and contaminant transport of a walking human, J. Fluids Eng. 127 (2005) 967–977.
[14] J.I. Choi, J.R. Edwards, Large eddy simulation and zonal modeling of human-induced contaminant transport, Indoor Air 18 (2008) 233–249.
[15] S.B. Poussou, M.W. Plesniak, Vortex dynamics and scalar transport in the wake of a bluff body driven through a steady recirculating flow, Exp. Fluids 53 (2012) 747–763.
[16] Y. Wu, N. Gao, The dynamics of the body motion induced wake flow and its effects on the contaminant dispersion, Build. Environ. 82 (2014) 63–74.
[17] B.H. Shaw, Heat and Mass Transfer by Convection through Large Rectangular Openings in Vertical Partitions [PhD thesis], Univ. Glasgow, United Kingdom, 1976, http://theses.gla.ac.uk/1975/.
[18] C.S. Hayden II, O.E. Johnston, R.T. Hughes, P.A. Jensen, Air volume migration from negative pressure isolation rooms during entry/exit, Appl. Occup. Environ. Hyg. 13 (1998) 518–527.
[19] J.W.-T. Tang, A. Nicolle, J. Pantelic, C.A. Klettner, R. Su, P. Kalliomäki, P. Saarinen, H. Koskela, K. Reijula, P. Mustakallio, D.K.W. Cheong, C. Sekhar, K.W. Tham, Different types of door-opening motion as contributing factors to containment failures in hospital isolation rooms, PLoS One 8 (2013) e66663, http://dx.doi.org/10.1371/journal.pone.0066663.
[20] P. Kalliomäki, P. Saarinen, J.W.-T. Tang, H. Koskela, Airflow patterns through single hinged and sliding doors in hospital isolation rooms, Int. J. Vent. 14 (2015) 111–126.
[21] J. Hang, Y. Li, W.H. Ching, J. Wei, R. Jin, L. Liu, X. Xie, Potential airborne transmission between two isolation cubicles through a shared anteroom, Build. Environ. 89 (2015) 264–278.
[22] A. Hathway, I. Papakonstantis, A. Bruce-Konuah, W. Brevis, Experimental and modelling investigations of air exchange and infection transfer due to hinged-door motion in office and hospital settings, Int. J. Vent. 14 (2015) 127–140.
[23] P. Saarinen, P. Kalliomäki, J.W.-T. Tang, H. Koskela, Large eddy simulation of air escape through a hospital isolation room single hinged doorway – validation by using tracer gases and simulated smoke videos, PLoS One 10 (2015) e0130667, http://dx.doi.org/10.1371/journal.pone.0130667.
[24] L. Fontana, A. Quintino, Experimental analysis of the transport of airborne contaminants between adjacent rooms at different pressure due to the door opening, Build. Environ. 81 (2014) 81–91.
[25] A. Kokkonen, M. Hyttinen, R. Holopainen, K. Salmi, P. Pasanen, Performance testing of engineering controls of airborne infection isolation rooms by tracer gas techniques, Indoor Built Environ. 23 (2014) 994–1001.
[26] J.I. Choi, J.R. Edwards, Large-eddy simulation of human-induced contaminant transport in room compartments, Indoor Air 22 (2012) 77–87.
[27] W.T. Leung, G.N. Sze-To, C.Y.H. Chao, S.C.T. Yu, J.K.C. Kwan, Study on the interzonal migration of airborne infectious particles in an isolation ward using benign bacteria, Indoor Air 23 (2012) 148–161.
[28] N.J. Adams, D.L. Johnson, R.A. Lynch, The effect of pressure differential and care provider movement on airborne infectious isolation room containment effectiveness, Am. J. Infect. Control 39 (2011) 91–97.
[29] I. Eames, D. Shoaib, C.A. Klettner, V. Taban, Movement of airborne contaminants in a hospital isolation room, J. R. Soc. Interface 6 (2009) S757–S766.
[30] Y-C. Shih, C-C. Chiu, O. Wang, Dynamic airflow simulation within an isolation room, Build. Environ. 42 (2006) 3194–3209.
[31] L. Chang, X. Zhang, S. Wang, J. Gao, Control room contaminant inleakage produced by the door opening and closing: dynamic simulation and experiments, Build. Environ. 98 (2016) 11–20.
[32] E.S. Mousavi, K.R. Grosskopf, Airflow patterns due to door motion and pressurization in hospital isolation rooms, Sci. Technol. Built Environ. (2016) 1–6, http://dx.doi.org/10.1080/23744731.2016.1155959.
[33] J.P. Rydock, P.K. Eian, Containment testing of isolation rooms, J. Hosp. Infect. 57 (2004) 228–232.
[34] S. Lee, B. Park, T. Kurabuchi, Numerical evaluation of influence of door opening on interzonal air exchange, Build. Environ. 102 (2016) 230–242.
[35] W.C. Beck, A test clean-room for evaluating contamination, Guthrie Clin. Bull. 36 (1966) 40.
[36] G. Baird, W. Whyte, Air movement control for treatment and isolation rooms, J. Hyg. 67 (1969) 225–232.
[37] K.W.D. Cheong, S.Y. Phua, Development of ventilation design strategy for effective removal of pollutant in the isolation room of a hospital, Build. Environ. 41 (2006) 1161–1170.
[38] H. Qian, Y. Li, Removal of exhaled particles by ventilation and deposition in a multibed airborne infection isolation room, Indoor Air 20 (2010) 284–297.
[39] Product document, Pro Smoke Super (ZR Mix) Fluid, Martin, Particle Size,

Fluid Density and Refractive Index Values, Revision A. http://www.martin.com/en-us/support/technical-note?file=/files/files/productdocuments/90_HINTS/999/techdoc_8074.html&returncontent=-true&Prodnumber=97120021&title=Particle Size, Fluid Density and Refractive Index Values, (accessed 29.3.16.).
[40] A.J. Smits, T.T. Lim (Eds.), Flow Visualization: Techniques and Examples, World Scientific, 2000. ISBN 1908977183.
[41] M. Lidwell, Air exchange through doorway. The effect of temperature difference, turbulence and ventilation flow, J. Hyg. 79 (1977) 141–154.
[42] P. Saarinen P. Kalliomäki, J.W-T. Tang, H. Koskela, The simulation of air migration through an isolation room doorway during passage. In Proceedings of Roomvent 2014, 13th International Conference on Air Distribution in Rooms, 19–22 October, Sao Paolo, Brazil.
[43] H.K. Kim, G. Augenbroe, Decision support for choosing ventilation operation strategy in hospital isolation rooms: a multi-criterion assessment under uncertainty, Build. Environ. 60 (2013) 305–318.
[44] M. Mattson M. Sandberg, Velocity field created by moving objects in rooms. In Proceedings of Roomvent 1996, 5th International Conference on Air Distribution in Rooms, 17–19 July, Yokohama, Japan.
[45] E. Bjørn, M. Mattsson, M. Sandberg, P.V. Nielsen, Displacement Ventilation: Effects of Movement and Exhalation, vol. 70, Univ. Aalborg, Dept. of Building Technology and Structural Engineering,Indoor Environmental Technology, 1997. V. R9728.
[46] A. Hathway, C. Noakes, P. Sleigh, L. Fletcher, CFD simulation of airborne pathogen transport due to human activities, Build. Environ. 46 (2011) 2500–2511.
[47] S.B. Poussou, Experimental Investigation of Airborne Contaminant Transport by a Human Wake Moving in a Ventilated Aircraft Cabin. [PhD thesis], Purdue Univ., West Lafayette, IN, USA.
[48] S.B. Poussou, M.W. Plesniak, Flow field in the wake of a bluff body driven through a steady recirculating flow, Exp. Fluids 56 (2015) 40.
[49] J. Hang, Y. Li, R. Jin, The influence of human walking on the flow and airborne transmission in a six-bed isolation room: tracer gas simulation, Build. Environ. 77 (2014) 119–134.
[50] Z.Y. Han, W.G. Weng, Q.Y. Huang, M. Fu, J. Yang, N. Luo, Aerodynamic characteristics of human movement behaviors in full-scale environment: comparison of limbs pendulum and body motion, Indoor Built Environ. 24 (2015) 87–100.
[51] Z.M. Moyer, The Human Aerodynamic Wake and the Design of a Portal to Sample It, Master's thesis, The Pennsylvania State University, Pennsylvania, USA, 2003.
[52] D. Licina, A. Melikov, C. Sekhar, K.W. Tham, Human convective boundary layer and its interaction with room ventilation flow, Indoor Air 25 (2015) 21–35, http://dx.doi.org/10.1111/ina.12120.
[53] C. Chen, B. Zhao, X. Yang, Y. Li, Role of two-way airflow owing to temperature difference in severe acute respiratory syndrome transmission: revisiting the largest nosocomial severe acute respiratory syndrome outbreak in Hong Kong, J. R. Soc. Interface 8 (2010) 699–710.
[54] D.E. Kiel, D.L. Wilson, Combining door swing pumping with density driven flow, ASHRAE Trans. 95 (1989) 590–599.